

A Miniaturised Neuromorphic Tactile Sensor integrated with an Anthropomorphic Robot Hand.

Benjamin Ward-Cherrier¹, Jörg Conradt², Manuel G. Catalano³, Matteo Bianchi⁴, Nathan F. Lepora¹

Abstract—Restoring tactile sensation is essential to enable in-hand manipulation and the smooth, natural control of upper-limb prosthetic devices. Here we present a platform to contribute to that long-term vision, combining an anthropomorphic robot hand (QB SoftHand) with a neuromorphic optical tactile sensor (neuroTac). Neuromorphic sensors aim to produce efficient, spike-based representations of information for bio-inspired processing. The development of this 5-fingered, sensorized hardware platform is validated with a customized mount allowing manual control of the hand. The platform is demonstrated to successfully identify 4 objects from the YCB object set, and accurately discriminate between 4 directions of shear during stable grasps. This platform could lead to wide-ranging developments in the areas of haptics, prosthetics and telerobotics.

I. INTRODUCTION

The sense of touch in humans allows us to interact with the environment, and is also an essential component for human social interaction [1] and in-hand object manipulation [2]. As such, restoring tactile sensation to users of prosthetic and telerobotic devices seems essential to provide a highly functional and intuitive user experience.

A key step to achieve this long-term goal is the development of accurate tactile sensors [3] able to capture relevant contact information. We suggest that neuromorphic sensors, which produce spike-based representations of information for efficient, bio-inspired processing, are ideally suited to the task.

Most neuromorphic sensors currently consist of event-based vision systems [4], [5]. In past work [6], we proposed the combination of these vision systems with the TacTip [7], an optical tactile sensor able to perform tactile tasks such as slip detection [8] and contour following [9]. Here, we further develop the neuroTac sensor, miniaturising and adapting it for use with the QB SoftHand.

BW was supported by a University of Bristol Vice-Chancellor's fellowship and NL was supported in part by a Leverhulme Trust Research Leadership Award on 'A biomimetic forebrain for robot touch' (RL-2016-039). This work has received funding from the European Unions Horizon 2020 Research and Innovation Programme (H2020-ICT-2019-2/ 2019-2023) under grant agreement No. 871237 (SOPHIA), and from the Italian Ministry of Education and Research (MIUR) in the framework of the CrossLab project (Departments of Excellence), and PRIN (Programmi di Ricerca Scientifica di Rilevante Interesse Nazionale) 2017 with the project TIGHT: Tactile InteGration for Humans and arTificial systems.

¹ BW and NL are with the Dept. of Engineering Mathematics, University of Bristol and Bristol Robotics Laboratory, University of Bristol, UK.

² JC is with the School of Electrical Engineering and Computer Science, KTH Royal Institute of Technology, Sweden.

³ MGC is with Istituto Italiano di Tecnologia, Genova, Italia.

⁴ MB is with the Centro di Ricerca E. Piaggio e Dipartimento di Ingegneria dell'Informazione, Università di Pisa, Pisa, Italia.

Corresponding author: b.ward-cherrier@bristol.ac.uk



Fig. 1: The QB SoftHand with an integrated neuromorphic optical tactile sensor. The neuroTac is integrated with the hand's index finger.

The QB SoftHand is a soft actuated, anthropomorphic robot hand based on adaptive synergies [10]. The hand features intuitive control and flexible grasps based on natural motions of the human hand.

Our aims in this paper are as follows:

- Miniaturise a neuromorphic optical tactile sensor and adapt it for use on the QB SoftHand, creating a hardware platform for the investigation of biomimetic tactile perception, haptic feedback and shared autonomy.
- Validate the sensor and its integration into the hand on an object recognition task and direction of shear detection task.

The performance of the sensor and its integration with the QB SoftHand is validated on an object recognition task, in which 4 objects from the YCB object set [11] are classified using a nearest-neighbour classification algorithm ($k=3$). The sensor is also shown to accurately identify within-grasp shear in 4 different directions with each of the 4 different objects.

II. BACKGROUND AND RELATED WORK

Closing the loop between action and perception involves three key aspects, according to Antfolk et al. [3]: (i) accurate sensors, (ii) reliable actuators and (iii) a tactile elicitation that allows an intuitive re-learning and adaptation of the Central Nervous System to the delivered inputs. Recent advances address point (ii) through the development of novel actuation methods [12], [13] and (iii) through non-invasive [14], [15] and invasive haptic feedback paradigms [16]. Here, we focus on point (i), the development of tactile sensors and their integration with robotic hands.

Robotic hands tend to be developed according to one of two design philosophies: highly complex anthropomorphic hands [17], or simple under-actuated robot hands and grippers [18]. The QB SoftHand utilised here combines these design philosophies as a five-fingered, under-actuated anthropomorphic hand. The QB SoftHand implements adaptive synergies [10] and soft actuation to enable a wide range of potential grasps from a single degree of actuation. Soft actuation introduces challenges when it comes to sensitizing the hand with tactile or proprioceptive capabilities, with classical solutions not being applicable due to the absence of rigid links. Proposed solutions have included the use of flexible strain sensors [19] in continuum soft robot hands and IMUs [15], [20] or motor encoder values [21] in soft articulated hands. Here our aim is to develop technologies and methods around neuromorphic sensing that could integrate with a soft articulated hand and lead to the sensitization of upper-limb prosthesis and telerobotics.

Neuromorphic engineering developed as a field in the late 1980s from work by Mead and colleagues [22] with the aim of replicating biological signal processing in electronic hardware [23]. The strong link to biology make neuromorphic technologies ideal candidates for integration with the human nervous system, as has been demonstrated with the creation and integration of artificial neuromorphic retinas [24]. We hypothesize that neuromorphic tactile sensors could be similarly developed to feed into the peripheral nervous system and restore a natural sense of touch to amputees [25].

As such, our interest here lies mainly in the creation of a neuromorphic tactile fingertip for integration with a prosthetic hand. Large-scale event-based tactile sensors such as those developed by Bergner et al. [26] or Lee et al. [27] have led to essential advances in event-based signal processing and architectures. These systems have demonstrated advantages in terms of speed and efficiency, and could enable the development of fully tactile robot skins. However our focus is on developing a platform for integration with a robotic hand, and thus our sensor's form factor should be approximately the size of a human fingertip.

Existing fingertip-sized neuromorphic tactile sensors include a sensor designed by Oddo et al. [28], [29] which combines analog outputs from 4 microelectromechanical sensors with an Izhikevich neuron model to produce a 16 taxel spike-based output. Crucially, this sensor is set up to mimic slowly adapting type 1 afferents, producing spikes

during constant pressure. Conversely, the neuroTac sensor is more akin to fast adapting type 1 afferents [30], transducing dynamic changes in the state of contact.

The miniaturised neuroTac sensor developed in this article is based on past work [6], which combines the design of the TacTip optical tactile sensor [7] with an event-based camera [5] to produce a spike-based output. Here, we use a miniaturised version of the camera [4] which has been successfully demonstrated on visual tasks such as 2d visual tracking [31], and integrate it in a human fingertip-sized tactile sensor for use with the QB SoftHand anthropomorphic hand.

III. METHODS

A. *The QB SoftHand*

The QB SoftHand (qbrobotics, QB SoftHand Research) is a commercial anthropomorphic robot hand based on the IIT/Pisa SoftHand [10]. The hand is designed using principles of soft robotics, with innovative flexible joints which are able to adapt to different object morphologies. The thumb is constructed with a hinge joint at its base enabling its flexion and extension, whereas the second, third, fourth and fifth digit comprise a base hinge joint which enables the fingers' abduction and adduction movement. Between the phalanges of each finger, a compliant rolling-contact element (CORE) joint comprising two coupled rolling cams guided by 3d-printed gears and elastic ligaments adds flexibility to the finger's trajectory during grasping. The flexibility inherent in the QB SoftHand's joint design makes it safe, robust and able to perform adaptable grasps, with nominal grasp forces of 62 N in the pinch configuration, and 84 N in the power grasp configuration (<https://qbrobotics.com/products/qb-soft-hand-research/>).

Another important aspect of the hand's construction is its reliance on adaptive synergies [32], a design method for underactuated hands which exploits the idea of motor primitives in human hand motion [33]. This method combined with mechanical compliance enables the QB SoftHand to be controlled through a single motor and single tendon system, yet be capable of a large number of grasps due to its intrinsic ability to adapt to object morphologies. The hand's single tendon runs in a loop from the palm through all five fingers, going up each finger through the CORE joints, around a pulley in each distal phalanx and then back towards the palm (for further technical details on the hand's design, see [10]).

Here, we use the QB SoftHand mounted on a device which attaches to a human user's arm and is powered by a battery (Parrot, ARDrone 2.0 1500mAh), allowing for self-contained operation. The hand is operated by the user through a lever which actuates the grasp when pulled, and returns to an open palm configuration when released.

B. *Integration of the neuroTac*

The neuroTac sensor was developed in previous work with a larger camera able to produce events and frames (iniVation, DAVIS240) [6] and is based on the design of a soft optical tactile sensor, the TacTip [7]. Although the neuroTac holds

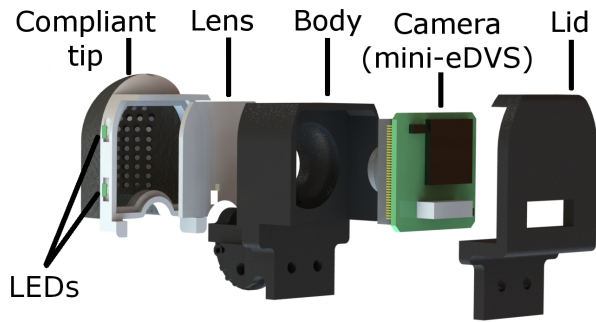


Fig. 2: Exploded CAD model of the neuroTac sensor. The event-based camera (mini-eDVS) captures movements of the pins in the compliant tip and transmits contact information in the form of precisely-timed spikes.

promise from an engineering perspective due to its speed and efficient representation of tactile data, we seek mostly to replicate and explore biological properties of touch in this artificial system. The neuroTac thus aims to emulate the structure of human skin through internal pins, and produces a spike-based output, mimicking mechanoreceptors in glabrous skin. Here, we miniaturise the design of the sensor and adapt it for integration with the QB SoftHand. The main contributions to hardware development are the following:

- Replacing the original event and frame-based camera [5] with a lower form factor, purely event-based camera, the mini-eDVS [4] with an adapted lens (developed by Conradt and colleagues).
- Adjusting the shape of the compliant tip from a hemispherical dome to mimic that of a human finger, with dimensions 20 mm (W) \times 25 mm (L) \times 30 mm (D). The hemispherical shape of the sensor is designed to ensure maximal coverage of the sensor during grasps.
- Redesigning the QB SoftHand’s distal phalanx to house a more compact pulley system, leaving room for the sensitized tip.

The sensor is made up of a 3d-printed fingertip-shaped compliant tip, with 79 internal markers mimicking the intermediate ridges in human glabrous skin. These markers are white-tipped inward extrusions of the 3d-printed skin which mechanically accentuate deformations. The number of markers is maximised within the limits of the 3d printer’s (Stratasys, Connex Objet 260) resolution. A 3d-printed rigid body and lid hold the event-based camera (mini-eDVS [4]), which produces events at the pixel level by thresholding changes in brightness (Fig. 2). The camera is made up of 128×128 pixels, with each pixel processing brightness changes in parallel at the hardware level and producing events in the address-event representation (AER) format. The threshold for these pixel events is manually set to capture displacements of the markers based on the sensor’s internal illumination.

The sensor outputs a series of precisely timed spikes ($\approx 1\mu\text{s}$ resolution) with spatial addresses corresponding to



Fig. 3: Objects used in the object recognition and shear detection experiments. Objects are from the YCB object set [11] and are labelled from left to right as “Racquetball”, “Tomato soup can”, “Box of sugar” and “Foam brick”.

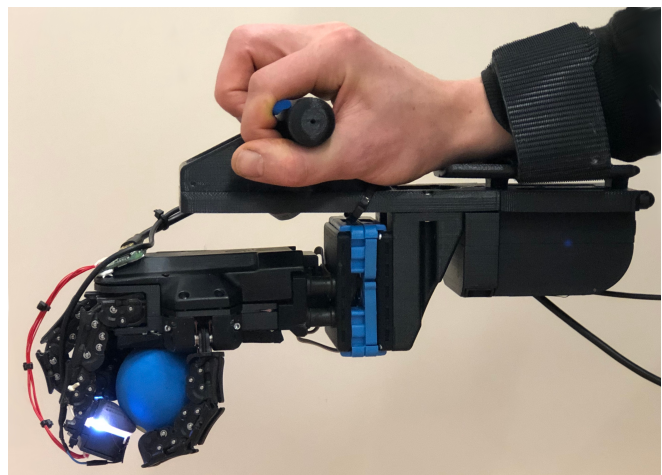


Fig. 4: Experimental setup for data collection. Objects are grasped by the QB SoftHand through the use of a hand-held, manually-controlled device attached to the experimenter’s arm.

their pixel location within the image. The neuroTac sensor is dynamic, in that it only outputs data when there is a change in contact conditions.

C. Experimental setup

We validate the sensor’s performance by testing it on two experiments: object recognition and shear detection. In both experiments, we use four objects from the YCB object set [11] chosen for their diverse materials and shapes (Fig. 3): a compliant rubber ball (labelled “Racquetball”), an empty metal can (labelled “Tomato Soup Can”), an empty cardboard box (labelled “Box of Sugar”) and a compliant brick made of soft foam (labelled “Foam Brick”).

Data is gathered from the sensitized QB SoftHand mounted on a hand-held device with manual grasp control (through the pull of a lever). In the object recognition condition, the hand is held palm upwards and objects placed by the experimenter in approximately the same in-hand

location for each grasp. In the shear condition, the device is held with a downwards facing open palm (Fig. 4), and perturbations correspond to a light push against the grasped object with one finger. Most investigations of artificial tactile sensing tend to operate in tightly-controlled environments with high precision robotic arms gathering data [7], [8], [34]. Here we are operating in a less controlled environment, and anticipate a larger presence of noise during data gathering. The aim here is to investigate the sensor’s performance in a more realistic scenario that could relate to prosthetics or tele-operation applications.

In the object recognition task, each object is grasped 20 times, with data recording being triggered approximately 1 second before the grasp is manually activated. Data is recorded over a 5 second period, capturing spikes over the full dynamic grasping motion. In the shear detection task, 20 runs of 5 second data trials are recorded for each of the 4 objects in each of the 4 directions of perturbation. Perturbations are defined as the experimenter gently pushing the grasped object with a finger of their free hand in one of four directions: Up (distal direction with relation to the palm), Down (proximal direction), Left (direction of adduction movement of the index) and Right (direction of abduction movement of the index). The resultant spikes are then processed and classified as described below.

D. Data processing and Classification

The data produced by the sensor for each trial is initially separated into $T = 64$ taxels indexed as $t = 1..64$ arranged in a 2d grid over the camera image. Each taxel is defined here as a region of the camera frame containing 16×16 pixels. The spikes produced within the taxel area are then accumulated over the trial duration (5 seconds here), and normalized by the total number of spikes over all pixels: N . This method effectively corresponds to the spatial coding method described in previous work [6], and results in an array of 64 integers, R_t , representing the spatial distribution of spikes across taxel areas.

$$R_t = \frac{\sum_{p_t} n_p}{N} \quad (1)$$

where the index $t = 1, \dots, 64$ represents taxel identity, p_t is the set of pixels belonging to taxel t , n_p denotes the number of spikes for pixel p and N is the total number of spikes over all pixels.

Data gathered consists of 80 trials (20 trials \times 4 classes) for each experimental condition, and is randomly split into training and testing sets according to an 80-20 split. Classification of object class and shear direction is performed in python through scikit-learn’s nearest neighbours algorithm (k=3) applied to processed data R_t , which assigns a class to each test sample based on its 3 closest training samples.

IV. RESULTS

A. Inspection of data

Data is gathered by grasping objects with the hand-held QB SoftHand device (Fig. 4). Due to the event-based nature

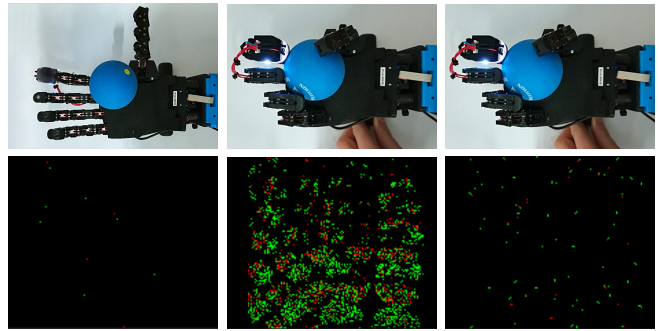


Fig. 5: Outputs of the sensor during an example grasp on the Racquetball object. The top row of figures show the three grasp phases, from left to right: pre-grasp, inception of grasp, completed grasp. The bottom row of figures show the output of the sensor during each phase, with events above the noise level occurring only during the inception of grasp phase.

of the mini-eDVS camera [4], the sensor outputs spikes only when a dynamic contact occurs.

The spike-based output of the sensor remains at a low level of activity resulting from noise during no-contact, and demonstrates high activity triggered by the movement of internal markers in the sensor during inception of contact. Post-contact, if the grasp is stable, the sensor returns to a low-activity mode, with bursts of spikes occurring during perturbation (Fig. 5). The two colours of events illustrated here correspond to ON events, when brightness increases above a given threshold (green events) and OFF events, when brightness decreases below a given threshold (red events). Although both types of events carry potentially relevant tactile information, we focus here on ON events for simplicity, and for their analogous nature to excitatory spikes in the human nervous system. Spikes are processed by separating the image into a 2d grid of 64 spatially distinct 16×16 pixel regions denoted taxels and accumulating spike activity over each taxel as described in section III-D.

B. Object recognition

Our initial validation of the sensor involves a test of within-grasp object recognition capabilities. This task is challenging since the hand’s inherent flexibility combined with our data acquisition method (Section III-C) can result in variable grasping configurations for the same object.

Classification of the four objects is performed by separating the camera’s pixels into a grid of 16×16 pixel regions, deemed taxels, and accumulating the spikes at each taxel over a 5s period for a given grasp (Fig. 6, Middle row). These taxel-wise spike counts are then normalised by the total number of spikes across the sensor, to obtain the relative spike rates of each taxel during the grasp (Fig. 6, Bottom row).

The taxel-wise spike distribution data is classified using an 80-20 train-test split and a nearest neighbours classifier, with k=3 using python’s scikit-learn module. This results in a perfect classification accuracy, as illustrated in the confusion matrix (Fig. 7) .

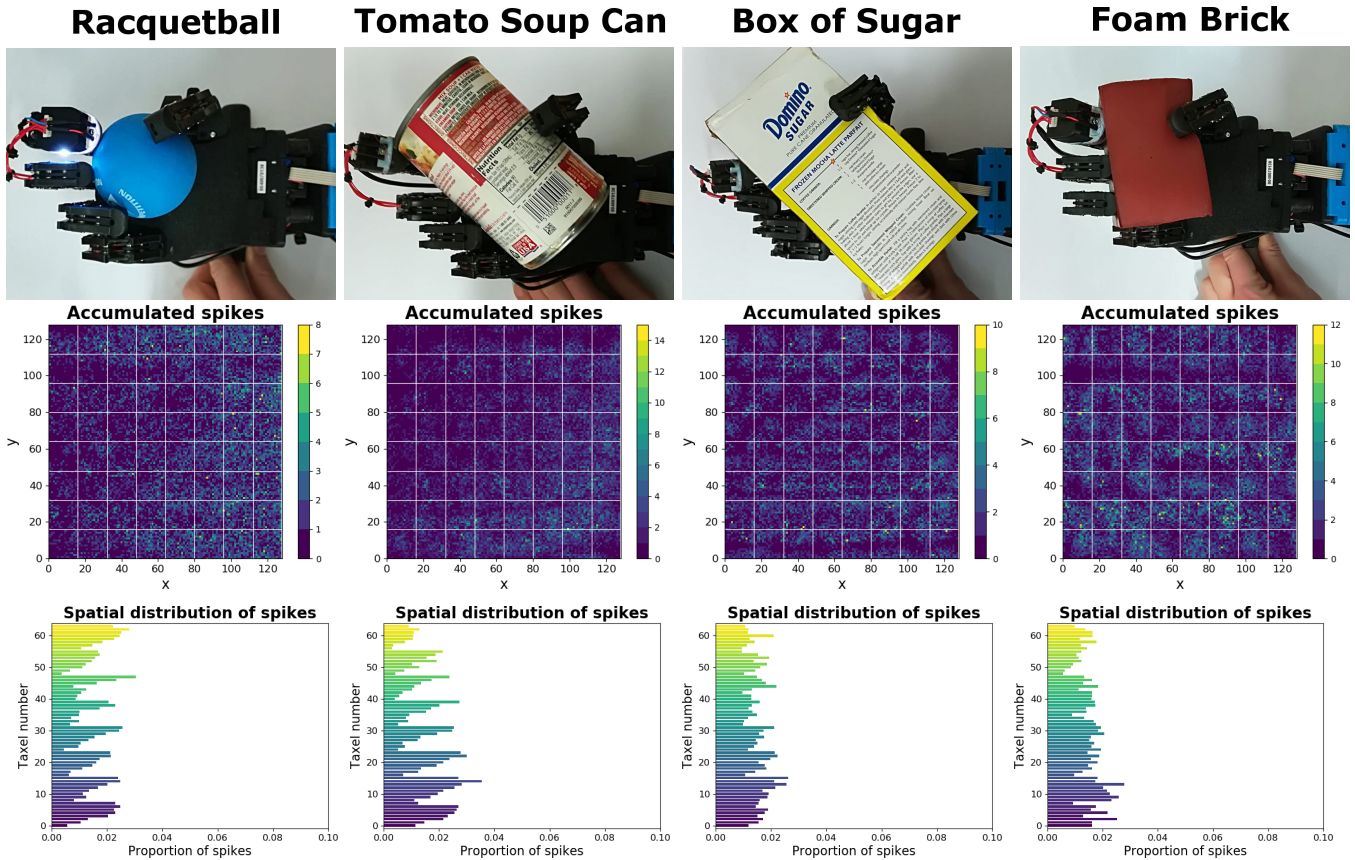


Fig. 6: Processing of spikes for classification in the object recognition task. Each column corresponds to one of the objects, from left to right: Racquetball, Tomato Soup Can, Box of Sugar, Foam Brick. Top row: Objects being grasped. Middle Row: Pixel-wise accumulation of spikes over the grasp duration and separation of the image into taxels. Bottom row: Proportional distribution of spikes over the taxel locations.

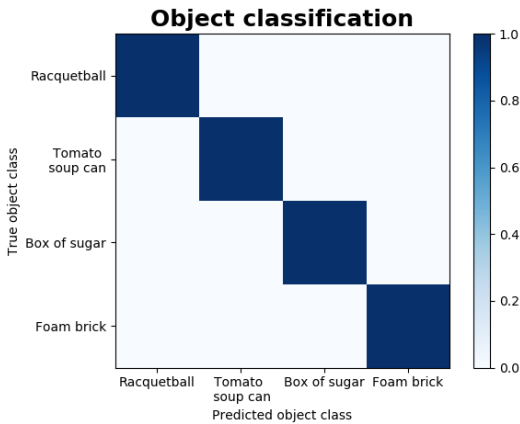


Fig. 7: Confusion matrix of the object classification task with a KNN classifier ($k=3$) on the spatial distribution of spikes.

These results are promising, but considering the objects are quite distinct in their shape and compliance characteristics, perhaps not surprising. We predict that the identification of more similar objects, such as balls of different dimensions, may require the integration of additional neuroTac sensors on the QB SoftHand.

C. Shear detection

Next, we investigate the sensor’s potential to detect and identify a perturbation occurring during a stable grasp. Perturbations are defined as pushing the grasped object with a finger in one of four directions: Up, Down, Left and Right. Up is defined as the distal direction with relation to the palm, and Down is the proximal direction, Left is the direction of adduction movement of the index and Right is the direction of its abduction movement (Fig. 8, leftmost panel).

Initial data gathered with the sensor while grasping the Racquetball object (Fig. 8, four rightmost panels) seems to indicate distinct signatures for each shear direction. The horizontal lines of pixel events appearing in the Up/Down directions and vertical lines in the Left/Right directions capture the movement of rows or columns of internal markers, respectively. We hypothesize that these characteristic spatial layouts of pixel events will enable the identification of within-grasp shear direction by the neuroTac sensor.

To verify this claim, we gather 20 runs of data in each of the 4 shear directions with all 4 objects. We then apply the same processing procedure as for object recognition, creating normalised taxel-wise spike counts over the sensor image (Sec. III-D), and classify shear direction independently for each object. We use an 80-20 train-test split with a nearest

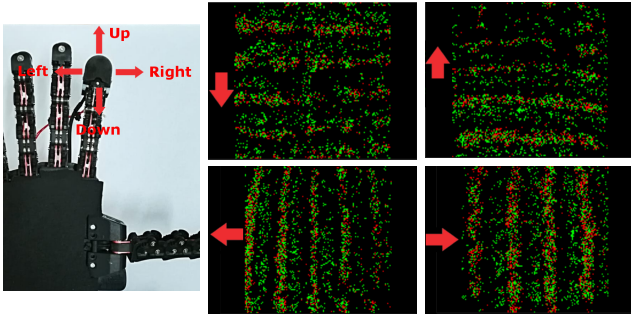


Fig. 8: Outputs of the sensor during grasp perturbations on the Racquetball object. The perturbations correspond to pushing the grasped object in one of four directions, shown in the left-most panel. The four images to the right show the sensor’s output for each direction of perturbation (as indicated by the red arrows).

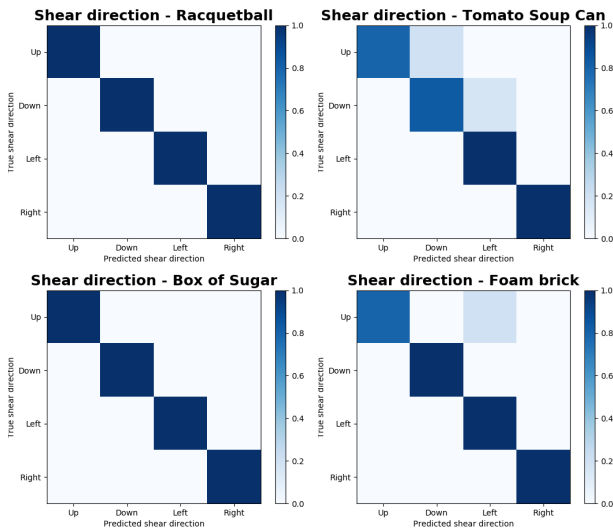


Fig. 9: Confusion matrices for the shear direction identification task for all 4 objects. Top Left: Racquetball, Top Right: Tomato Soup Can, Bottom Left: Box of Sugar, Bottom Right: Foam Brick. We use a nearest neighbour classifier ($k=3$) on the spatial distribution of spikes to identify the direction of shear.

neighbour classifier ($k=3$).

Results show an overall strong performance on the classification of shear direction (Fig. 9), with perfect accuracy for the Racquetball and Box of Sugar objects, and near perfect accuracy for the Tomato Soup Can (93.75%) and Foam Brick (97.5%) objects. Misclassification of these objects likely results from variations in the direction and force exerted during perturbation of the grasp.

V. DISCUSSION

In this paper, we presented the integration of the neuroTac sensor with the QB SoftHand. The performance of the neuroTac and its integration with the hand is validated on two tasks involving 4 objects from the YCB object set [11]. Both experiments involve classification of the taxel-wise

accumulated spikes by a nearest neighbour algorithm ($k = 3$). The first task is the classification of grasped objects, showing perfect accuracy over this restricted set of objects. The second task is the identification of a direction of perturbation of the object from within the grasp. We demonstrate the sensor is able to accurately identify shear direction within the hand’s grasp for the 4 different objects.

The platform developed here combines the adaptive, versatile grasping and simple control of the QB SoftHand with dynamic, spike-based contact information from the neuroTac sensor. The question of how best to process neuromorphic data is an unsolved problem, however for prosthetic or telerobotic applications, tactile information from the neuroTac sensor should be used in ways that minimise cognitive load on the user, in keeping with the QB SoftHand’s focus on intuitive control.

Areas of further development could include an updated design of the mechanical joint in the sensitized phalanx to reduce friction on the tendon. Additional sensors could also be integrated into the hand, which would likely provide a more complete picture of grasp contact for more complex tactile tasks. Finally, the processing method used here to validate the sensor focuses on the spatial distribution of spikes, akin to a biological rate code [35]. Recent theories in neuroscience hold that the representation of spike times as a rate code, though appealing because of its simplicity, does not capture the full spectrum of information conveyed by neural codes [36]. Alternative coding strategies have been suggested that take into account the precise or relative timing of spikes, such as rank order coding [37]. Future studies with the neuroTac could implement these methods to explore more biologically plausible somatosensory processing, as well as considering OFF events which provide additional information on shear and object shape.

Here we have demonstrated the integration of the neuroTac sensor with the QB SoftHand, and its application to a simple object recognition task and shear direction detection task. This platform shows promise for applications to prosthetics and telerobotics, with the adaptive grasping of the QB SoftHand allowing for versatile grasping of irregular objects, and the sensor’s comprehensive biomimetic output being highly suited for future implementations of shared autonomy protocols, in which embedded intelligence within the hand performs reflex-like actions while haptic feedback is provided to the user.

VI. CONCLUSION

We presented a platform comprising a neuromorphic optical tactile sensor (neuroTac) integrated with a soft articulated anthropomorphic robot hand (qrobotics, QB SoftHand). The system was validated on two tasks, demonstrating successful object recognition and accurate detection of in-hand shear direction. The hardware developed presents a combination of intuitive control and neuromorphic dynamic contact information, and could lead to wide-ranging developments in the areas of haptics, prosthetics and telerobotics.

Acknowledgements: We thank Andrew Stinchcombe and John Lloyd for help with hardware development.

REFERENCES

- [1] R. Dunbar. The social role of touch in humans and primates: behavioural function and neurobiological mechanisms. *Neuroscience & Biobehavioral Reviews*, 34(2):260–268, 2010.
- [2] H. Yousef, M. Boukallel, and K. Althoefer. Tactile sensing for dexterous in-hand manipulation in robotics—a review. *Sensors and Actuators A: physical*, 167(2):171–187, 2011.
- [3] C. Antfolk, M. Dalonzo, B. Rosén, G. Lundborg, F. Sebelius, and C. Cipriani. Sensory feedback in upper limb prosthetics. *Expert review of medical devices*, 10(1):45–54, 2013.
- [4] P. Lichtsteiner, C. Posch, and T. Delbruck. A 128x128 120 db 15 μs latency asynchronous temporal contrast vision sensor. *IEEE journal of solid-state circuits*, 43(2):566–576, 2008.
- [5] C. Brandli, R. Berner, M. Yang, S. Liu, and T. Delbruck. A 240×180 130 db 3 μs latency global shutter spatiotemporal vision sensor. *IEEE Journal of Solid-State Circuits*, 49(10):2333–2341, 2014.
- [6] B. Ward-Cherrier, N. Pestell, and N. Lepora. Neurotac: A neuromorphic optical tactile sensor applied to texture recognition. *arXiv preprint arXiv:2003.00467*, 2020.
- [7] B. Ward-Cherrier, N. Pestell, L. Cramphorn, B. Winstone, M. Giannaccini, J. Rossiter, and N. Lepora. The tactip family: Soft optical tactile sensors with 3d-printed biomimetic morphologies. *Soft robotics*, 5(2):216–227, 2018.
- [8] J. James, N. Pestell, and N. Lepora. Slip detection with a biomimetic tactile sensor. *IEEE Robotics and Automation Letters*, 3(4):3340–3346, 2018.
- [9] N. Lepora, A. Church, C. De Kerckhove, R. Hadsell, and J. Lloyd. From pixels to percepts: Highly robust edge perception and contour following using deep learning and an optical biomimetic tactile sensor. *IEEE Robotics and Automation Letters*, 4(2):2101–2107, 2019.
- [10] Manuel G Catalano, Giorgio Grioli, Edoardo Farnioli, Alessandro Serio, Cristina Piazza, and Antonio Bicchi. Adaptive synergies for the design and control of the pisa/iit sofhand. *The International Journal of Robotics Research*, 33(5):768–782, 2014.
- [11] B. Calli, A. Singh, A. Walsman, S. Srinivasa, P. Abbeel, and A. Dollar. The ycb object and model set: Towards common benchmarks for manipulation research. In *2015 international conference on advanced robotics (ICAR)*, pages 510–517. IEEE, 2015.
- [12] K. Andrianesis and A. Tzes. Design of an anthropomorphic prosthetic hand driven by shape memory alloy actuators. In *2008 2nd IEEE RAS & EMBS International Conference on Biomedical Robotics and Biomechatronics*, pages 517–522. IEEE, 2008.
- [13] E. Biddiss and T. Chau. Dielectric elastomers as actuators for upper limb prosthetics: Challenges and opportunities. *Medical engineering & physics*, 30(4):403–418, 2008.
- [14] F. Clemente, M. D’Alonzo, M. Controzzi, B. Edin, and C. Cipriani. Non-invasive, temporally discrete feedback of object contact and release improves grasp control of closed-loop myoelectric transradial prostheses. *IEEE Transactions on Neural Systems and Rehabilitation Engineering*, 24(12):1314–1322, 2015.
- [15] S. Fani, K. Di Blasio, M. Bianchi, M. Catalano, G. Grioli, and A. Bicchi. Relaying the high-frequency contents of tactile feedback to robotic prosthesis users: Design, filtering, implementation, and validation. *IEEE Robotics and Automation Letters*, 4(2):926–933, 2019.
- [16] K. Kim and E. Colgate. Haptic feedback enhances grip force control of semg-controlled prosthetic hands in targeted reinnervation amputees. *IEEE Transactions on Neural Systems and Rehabilitation Engineering*, 20(6):798–805, 2012.
- [17] Z. Xu and E. Todorov. Design of a highly biomimetic anthropomorphic robotic hand towards artificial limb regeneration. In *2016 IEEE International Conference on Robotics and Automation (ICRA)*, pages 3485–3492. IEEE, 2016.
- [18] R. Ma and A. Dollar. Yale openhand project: Optimizing open-source hand designs for ease of fabrication and adoption. *IEEE Robotics & Automation Magazine*, 24(1):32–40, 2017.
- [19] V. Wall and O. Brock. Multi-task sensorization of soft actuators using prior knowledge. In *2019 International Conference on Robotics and Automation (ICRA)*, pages 9416–9421. IEEE, 2019.
- [20] G. Santaera, E. Luberto, A. Serio, M. Gabicchini, and A. Bicchi. Low-cost, fast and accurate reconstruction of robotic and human postures via imu measurements. In *2015 IEEE International Conference on Robotics and Automation (ICRA)*, pages 2728–2735. IEEE, 2015.
- [21] E. Battaglia, J. Clark, M. Bianchi, M. Catalano, A. Bicchi, and M. O’Malley. The rice haptic rocker: skin stretch haptic feedback with the pisa/iit sofhand. In *2017 IEEE World Haptics Conference (WHC)*, pages 7–12. IEEE, 2017.
- [22] C. Mead. Neuromorphic electronic systems. *Proceedings of the IEEE*, 78(10):1629–1636, 1990.
- [23] M. Mahowald and R. Douglas. A silicon neuron. *Nature*, 354(6354):515–518, 1991.
- [24] K. Zaghoul and K. Boahen. A silicon retina that reproduces signals in the optic nerve. *Journal of neural engineering*, 3(4):257, 2006.
- [25] S. Raspopovic, M. Capogrosso, F. Petrini, M. Bonizzato, J. Rigosa, G. Di Pino, J. Carpaneto, M. Controzzi, T. Boretius, E. Fernandez, et al. Restoring natural sensory feedback in real-time bidirectional hand prostheses. *Science translational medicine*, 6(222):222ra19–222ra19, 2014.
- [26] F. Bergner, P. Mittendorfer, E. Dean-Leon, and G. Cheng. Event-based signaling for reducing required data rates and processing power in a large-scale artificial robotic skin. In *2015 IEEE/RSJ International Conference on Intelligent Robots and Systems (IROS)*, pages 2124–2129. IEEE, 2015.
- [27] W. Lee, S. Kukreja, and N. Thakor. A kilohertz kilotaxel tactile sensor array for investigating spatiotemporal features in neuromorphic touch. In *2015 IEEE Biomedical Circuits and Systems Conference (BioCAS)*, pages 1–4. IEEE, 2015.
- [28] G. Spigler, C. Oddo, and M. Carrozza. Soft-neuromorphic artificial touch for applications in neuro-robotics. In *2012 4th IEEE RAS & EMBS international conference on biomedical robotics and biomechanics (BioRob)*, pages 1913–1918. IEEE, 2012.
- [29] C. Oddo, L. Beccai, M. Felder, F. Giovacchini, and M. Carrozza. Artificial roughness encoding with a bio-inspired mems-based tactile sensor array. *Sensors*, 9(5):3161–3183, 2009.
- [30] R. Johansson and R. Flanagan. Coding and use of tactile signals from the fingertips in object manipulation tasks. *Nature Reviews Neuroscience*, 10(5):345–359, 2009.
- [31] G. Müller and J. Conradt. A miniature low-power sensor system for real time 2d visual tracking of led markers. In *2011 IEEE International Conference on Robotics and Biomimetics*, pages 2429–2434. IEEE, 2011.
- [32] Giorgio Grioli, Manuel Catalano, Emanuele Silvestro, Simone Tono, and Antonio Bicchi. Adaptive synergies: an approach to the design of under-actuated robotic hands. In *2012 IEEE/RSJ International Conference on Intelligent Robots and Systems*, pages 1251–1256. IEEE, 2012.
- [33] E. Weiss and M. Flanders. Muscular and postural synergies of the human hand. *Journal of neurophysiology*, 92(1):523–535, 2004.
- [34] W. Yuan, R. Li, M. Srinivasan, and E. Adelson. Measurement of shear and slip with a gelsight tactile sensor. In *2015 IEEE International Conference on Robotics and Automation (ICRA)*, pages 304–311. IEEE, 2015.
- [35] S. Thorpe, A. Delorme, and R. Van Rullen. Spike-based strategies for rapid processing. *Neural networks*, 14(6-7):715–725, 2001.
- [36] E. Mackevicius, M. Best, H. Saal, and S. Bensmaia. Millisecond precision spike timing shapes tactile perception. *Journal of Neuroscience*, 32(44):15309–15317, 2012.
- [37] J. Gautrais and S. Thorpe. Rate coding versus temporal order coding: a theoretical approach. *Biosystems*, 48(1-3):57–65, 1998.